Sensors & Transducers, Vol. 238, Issue 11, November 2019, pp. 72-79

Sensors & Transducers

Published by IFSA Publishing, S. L., 2019
http://www.sensorsportal.com

Tunable Separation of Nanoparticles in a Continuous Flow Using Standing Surface Acoustic Wave

[1, *] Amar CHAALANE, [1] Mahmoud ADDOUCHE, [2] Rabah ZEGGARI, [1] Daniel GUNEYSU, [1] Franck LARDET-VIEUDRIN, [3] Amine BERMAK, [1] Céline ELIE-CAILLE, [1] Wilfrid BOIREAU and [1] Abdelkrim KHELIF

[1] FEMTO-ST Institute, UBFC, CNRS, ENSMM, UTBM,
15B Avenue des Montboucons, 25030 Besançon, France
[2] FEMTO Engineering, 15B Avenue des Montboucons, 25030 Besançon, France
[3] College of Science and Engineering, Hamad Bin Khalifa University, Qatar Foundation,
Doha 5825, Qatar
[*] Tel.: +33(0)363082432, fax: +33(0)363082400
E-mail: amar.chaalane@femto-st.fr

Received: 30 August 2019 /Accepted: 15 October 2019 /Published: 30 November 2019

Abstract: Manipulating micro and nano-biological particles like extracellular vehicles (EVs), without extracting them from their biological media, presents a big challenge for diagnosis purposes. Here we present the design and fabrication of a sorting device based on the combination of microfluidic and electroacoustic modules that is capable of aligning and sorting submicron biological particles according to their size, compressibility or mass density, all in a tunable way. The device relies on a lithium niobate (LN) substrate to generate acoustic waves assembled with a micromachined glass layer for microfluidic circuits. The interference between the two surface acoustic waves (SAWs) generated by interdigitated transducers (IDTs) create a distribution of an acoustic radiation force (ARF). This force affects differently particles depending on their physical proprieties. The device is powered by an electronic circuit with a phase shifter to move the node of the standing surface acoustic wave (SSAW) along the channel width. When the device is powered at resonance frequency of the IDTs, experiment shows submicron particles alignment along the channel. By shifting the electrical signal between the two IDTs we can translate the pressure node at any targeted position in the channel width. The particles are then driven to one selected outlet.

Keywords: Nanotechnology, Microfluidic, Extracellular vesicles, Nanoparticles separation, Standing surface acoustic wave, Acoustic radiation force.

1. Introduction

The ability to sort, sieve, and manipulate small particles, especially in a tunable way, is highly required for various applications ranging from Micro-Nanoparticle sorting [1] to targeting drug delivery [2]. A conventional sieve uses a mesh of fixed size for separating smaller particles from the particle mixture of various sizes, but the limitation is that could not sort out different materials of the same size and is incapable of particle manipulation. Acoustic [3–8] and optical [9–13] tweezers have been developed to trap and manipulate nanoparticles [14-15], biomolecules [16-17], and organisms [18], yet they can capture only a few particles at a time and are difficult to scale up.

Otherwise, manipulating micro and nano-biological particles like extracellular vesicles (EVs), without extracting them from their biological media, presents a big challenge for the biological, clinical and pharmaceutical communities. Since EVs represents a highly important mediators in cell-to-cell communication [19–20], sorting and trapping them allows a better detection and qualification for diagnosis purposes.

Many technics have been used to improve the efficacy of particle sorting devices. In acoustic microfluidic devices, either bulk acoustic waves (BAWs) [21] or surface acoustic waves (SAWs) [22] are used to generate standing acoustic wave fields to trap particles realizing meso-scale particle patterning. This concept has become possible by the integration of acoustic and microfluidic systems in the same chip. It allows controlling the interaction between the acoustic wave and the submicron particles flowing in a channel of about tens microns wide.

In this work we introduce an acoustic sorting that can align, sort, and transfer a large number of particles in a liquid according to their physical proprieties (size, compressibility or mass density), all in a tunable manner. This device, based on the combination of microfluidic and electroacoustic systems, not only overcomes the shortfalls of a traditional sieve and acoustic or optical tweezers, but also fulfills many more functionalities.

The concept is motivated by the highly localized radiation force induced by the artificially engineered interdigitated (IDT) fingers patterned of a piezoelectric substrate to fulfill acoustic field. It is thus distinct from other acoustic techniques that rely on bulk standing waves or Gaussian beams directly generated by the acoustic transducer to trap one or several identical particles [3–8]. Such a resonance transmission and highly localized field in the region between the two IDTs induce a large acoustic radiation force that can be used to trap and sort small particles of few 100 nm of size. These techniques target to sort only one particle category (size range) at the same time. While in the device we will present in this paper, particles of different size can be gathered, at the same time, in several parallel lines where each line contains a distinct category in term of particle size.

2. Theoretical Analysis

When a particle in a viscous fluid interacts with a stationary elastic wave, two types of forces act on this particle: the acoustic force F_a and the Stokes forceF_{Stokes}. Since the acoustic force has a sinusoidal shape, it tends to move heavy and/or large size particles from the extremum towards the nodes. The Stokes force (so-called drag force) is a resistance force to the acoustic force.

The acoustic force F_a on a compressible and spherical particle can be expressed as [23]:

$$F_a = \frac{\pi^2 {P_a}^2 {R_p}^2}{3\lambda} \beta_f \, \phi(\beta,\rho) \sin\left(\frac{4\pi}{\lambda}x\right), \qquad (1)$$

where P_a is the acoustic pressure, R_p is the particle radius, β_f is the compressibility of the fluid, $\phi(\beta,\rho)$ is the acoustic contrast factor, λ is the acoustic standing wave wavelength and x is the particle position across the fluidic channel ($x = 0$ in the center of channel). The acoustic pressure is further determined from the device characteristics:

$$P_a = \sqrt{\frac{PZ}{A}}, \qquad (2)$$

where Z is the acoustic impedance of the substrate, A is the IDT area, and P is the power of the input signal. The mechanical properties of MVs are represented by the acoustic contrast factor:

$$\phi(\beta,\rho) = \left(\frac{5\rho_p - 2\rho_f}{2\rho_p + \rho_f}\right) - \left(\frac{\beta_p}{\beta_f}\right), \qquad (3)$$

where ρ and β are the density and the compressibility of the particle, respectively. The indexes p and f corresponds to the particle and the fluid, respectively.

In the case of micro/nano-vesicles flowing in a fluid buffer, $\phi(\beta,\rho)$ will be positive. Therefore, vesicles move toward the acoustic force node positions.

According to the symmetry of the SAW system, the initial position of the pressure node (without applying a phase-shift) is normally located on the SAW system symmetry line. Therefore, this position corresponds to the center of the microfluidic channel. A phase-shift between the electrical signals of excitation of the IDTs makes it possible to shift the node to any desired position over the width of the channel, in a tunable manner.

The second force is the Stokes force F_{Stokes}:

$$F_{Stokes} = -6\pi\eta R_p(u_p - u_f), \qquad (4)$$

where η is the dynamic viscosity of the fluid, R_p is the particle radius and u is the velocity. The indexes p and f corresponds to the particle and the fluid, respectively.

We obtain the motion characteristics of vesicles in a viscous flow by solving the equation:

$$F_a + F_{Stokes} = 0, \qquad (5)$$

that gives:

$$\frac{\pi^2 PZ {R_p}^2 \beta_f}{3\lambda A}\left[\left(\frac{5\rho_p - 2\rho_f}{2\rho_p + \rho_f}\right) - \left(\frac{\beta_p}{\beta_f}\right)\right]\sin\left(\frac{4\pi}{\lambda}x\right) - 6\pi\eta R_p(u_p - u_f) = 0 \qquad (6)$$

The acoustic force is proportional to the particle volume and the drag force to the particle diameter.

This means that larger vesicles move faster to the pressure nodes, while smaller vesicles continue to move along the channel, at their original positions of entry into the acoustic opening, very little affected by acoustic force. Smaller particles will be aligned at the bellies (extremums) positions because the larger particles push them away of the nodes.

Indeed, the transit time τ of MVs moving from the channel center to the sheath flow is $\sim 1/{R_p}^2$, which enables size-selective vesicles separation [23]. This is why, in our design, we fixed the acoustic aperture at 5.2 mm to be larger than the distance traveled by the particles in a time duration τ. In this configuration, we can be sure that the particle motion reaches the steady state regime before coming out of the acoustic zone.

3. Methodology: a Tunable Manner for Nanoparticle Manipulation

The principal of particles manipulation using SAW is to generate a standing wave starting from two traveling surface acoustic waves (TSAW) that propagates in two opposite directions. This SSAW drives the particle toward one targeted position in the channel center that correspond to the pressure node (cf. Fig. 1).

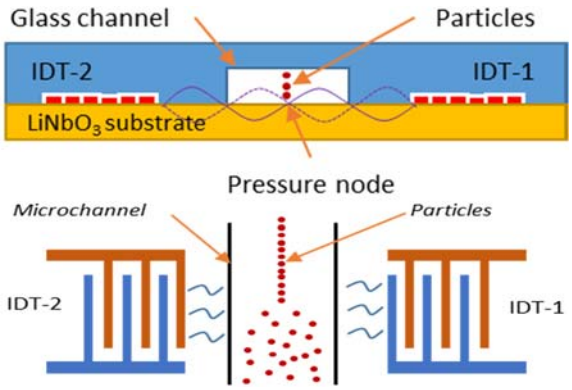

Fig. 1. Schematic of the acousto-fluidic device. It is composed of two IDTs patterned on piezoelectric substrate and a microchannel realized on glass substrate. The acoustic force drives larger vesicles to move faster to the pressure nodes, while smaller vesicles, very little affected, continue to move along the channel.

The standing wave occurred in the microchannel region generates an acoustic radiation force (ARF) that affects differently particles in fluid depending on their properties. The heavy and dense particles tend to tighten towards the nodes while the light and compressible particles remain on the antinodes [24-25]. This allow aligning the large size particles in the pressure node and the small size one in the anti-nodes.

The idea here is to manipulate the position of the aligned particles simply by a continuous variation of the electrical signal phase between the two IDTs. This allows translating the node of the standing wave from the channel center to any targeted position situated in the channel width. As so, we can align and drive particles toward one desired channel outlet among the other outlets of the microfluidic circuit. Fig. 2 shows MATLAB software simulations of the electrical phase shifting effect on the position of pressure node, and this for fours relative phase shifting angles of 0°; 60°; 120° and 180°.

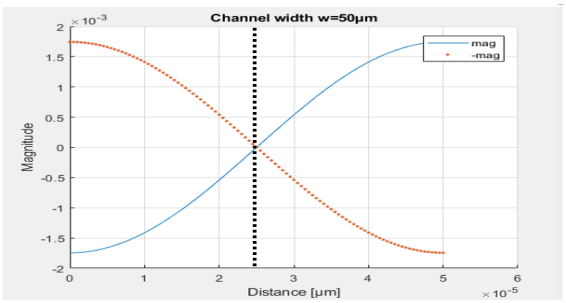

a) Δφ=0°

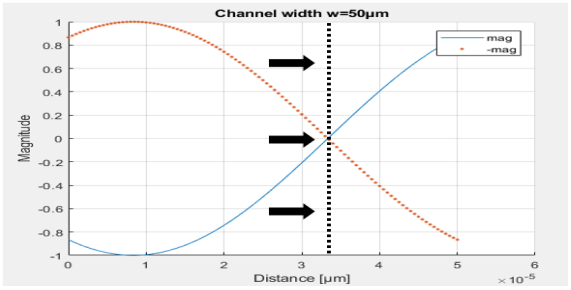

b) Δφ=60°

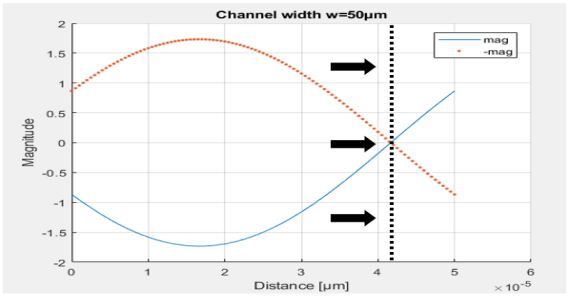

c) Δφ=120°

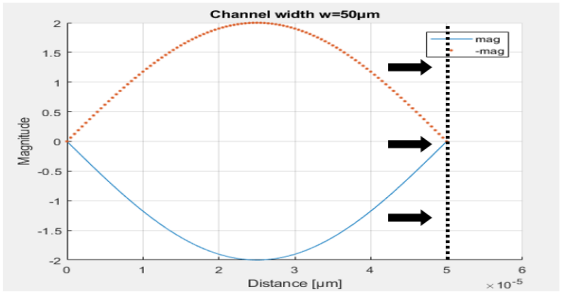

d) Δφ=180°

Fig. 2. Simulations of the tunable manner to translate the pressure node position from the center of the channel to the right wall, by shifting the electrical signal of 0°; 60°; 120° and 180°.

4. Experimental Results

4.1. Design and Geometrical Parameters

The design of the implemented acousto-fluidic system with the details of the microfluidic circuit and the network of fingers that compose the IDTs are presented in Fig. 3. It is composed of two layers of 3×3 cm^2 area: a glass layer for the microfluidic circuit and a piezoelectric layer for the acoustic wave generation.

The microfluidic circuit contains a main channel of l_c of length, w_c of width and h_c of depth, and six secondary channels. Each one of them ends on a circular hole that crosses the entire glass wafer thickness. Three holes are considered as "inlets" for the fluid injecting while the other three holes as "outlets" to recover either buffer or sorted particles.

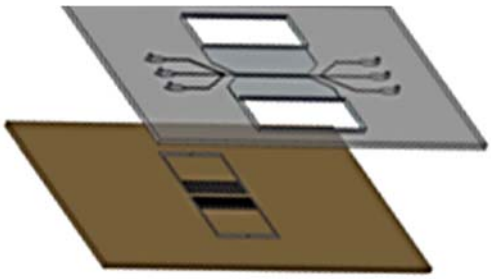

Fig. 3. A schematic view of the submicron particles separation micro-device with (top) the glass layer and (bottom) the piezoelectric layer. For the glass layer, we consider the three holes on the right side of as inlets while the other three holes as outlets for the fluidic.

The glass channel of 9 mm of length can be functionalized and coated to limit unwanted adsorptions. The use of glass allows a better biocompatibility, and a multi-use system. It is also to overcome limitation of PDMS for biology. Indeed, this elastomer ages, is sensitive to exposure at some chemicals and permeable enough to gas [26].

Two interdigital transducers (IDTs) are patterned on piezoelectric substrate of a lithium niobate ($LiNbO_3$). This material is very used for the manufacture of surface acoustic wave devices because of it high piezoelectric coupling factor. The two IDTs generate SSAW and thus acoustic force is created inside the channel. We fixed the width of the fluidic channel to 60 µm in order to match the acoustic half-wavelength. Based on the speed of sound of the SAW and the acoustic wavelength, the frequency of 40 MHz is used to supply the SAW transducers. In these conditions, the microchannel has one pressure node located at the center and two pressure anti-nodes located close to the walls. However, this position can be altered via a phase shift to any wanted position between the two IDTs.

The IDT electrode geometry is shown in Fig. 4, where the single-electrode-type (so-called solid-electrode-type) configuration has been adopted for the excitation of SAWs. The single-electrode-type IDT is widely used because of its structural simplicity and relatively wide strip width ($\sim \lambda/4$), which reduces the required resolution of photolithography [27].

The width w_e and pitch p_e of IDT electrodes are all 25 µm. This configuration generates SAW with wavelength λ of 100 µm. The distance between IDTs L is 700 µm. Because the behavior of SAW excitation at the IDT limit is somewhat different from that in its center region, the acoustic aperture W have to be large (here W = 5.2 mm); this is to avoid a significant diffraction effect of the traveling wave that take place in the IDT edge [27]. Furthermore, a larger aperture let a long nanoparticles-SSAW interaction time, allowing high flow particle sorting. The number of IDT finger-pairs (N=20) must be large enough to generate acoustic power capable of interacting with the nanoparticles but not very large to make the characteristics of IDT complex. This complexity is caused by the reflection of Bragg which occurs when $\lambda \sim p_e$ corresponding to the resonance condition for SAW excitation [27].

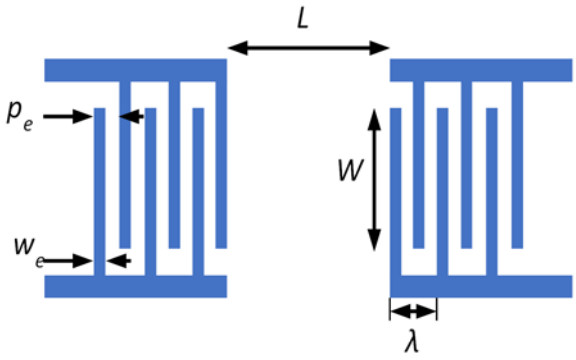

Fig. 4. Scheme of the SAW interdigitated transducer with the parameters of the electrode fingers.

4.2. Summary of the Fabrication Process

The acousto-fluidic device microfabrication process is mainly composed of three steps:

1) The realization of IDTs electrode onto a 128° Y-cut $LiNb0_3$ piezoelectric substrate.

2) The micro-machining of microfluidic circuit on a glass wafer: the wafer top side was micro-machined by deep reactive ion etching (DRIE) to achieve microchannels design. A femtosecond (FS) laser boring technic is used on the wafer backside to achieve holes of 500 µm in diameter for the fluidic inlets and outlets.

3) Both lithium niobate and glass wafers were stacked together in order to close the microfluidic circuit and to allow fluidic and acoustic interaction.

The realized SAW interdigitated transducer is presented in Fig. 5. It is composed of IDT-1 on the top and IDT-2 on the bottom, separates by the fluidic microchannel. The first wave propagates from top to down while the second one propagates in the opposite direction to fulfill a standing acoustic wave.

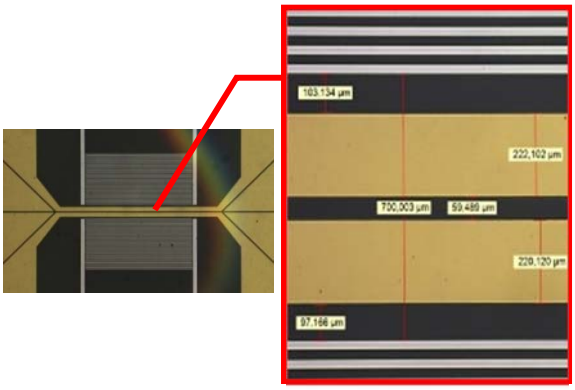

Fig. 5. The picture of the SAW interdigitated transducer that actuates with nanoparticles presents in a liquid. The last one is flowing in microchannel deposited on the $LiNbO_3$ substrate. The first wave propagates from top to down. The second one propagates in the opposite direction. The acoustic aperture is of 5.2 mm and the IDTs length is of 700 µm.

The microfluidic circuit is dry etched through a single step of photolithography until 30 µm of depth. Thus, the effective section of the channel is of trapezoidal shape with w_1=59.75 µm of width on the surface level and w_2=32.17 µm of width at the bottom level of the channel. Fig. 6 shows picture of the micro-acousto-fluidic device for nanoparticles manipulating and sorting.

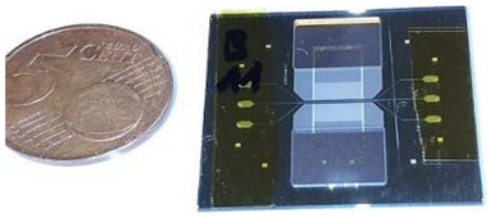

Fig. 6. A picture of the acousto-fluidic nanoparticles manipulator device. It is composed of a glass layer for the microfluidic circuit stacked to a lithium niobate layer for the acoustic standing wave.

4.3. Electrical Measurements

In order to characterize the microsystem, we have manufactured a mechanical support (Fig. 7) allowing to (1) host the device, (2) ensure the six fluidic connections to a controlled injection system and (3) connect IDTS for both the electrical characterization and SAW generation.

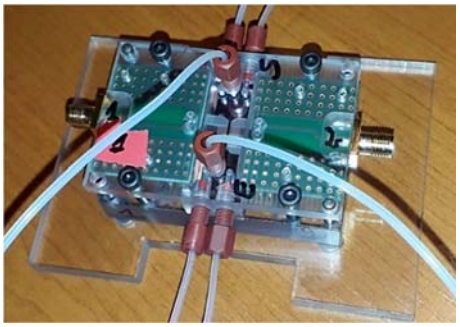

Fig. 7. The realized acousto-fluidic device with electric and microfluidic connections.

In Fig. 8 we represent a schematic view of the experimental setup. The device is powered by an AC sinusoidal signal generated by a, Anritsu 68147C synthesized signal generator. A power splitter divides the signal in two ways (0° and 180°) to supply the two IDTs. The first line (upper one) is used for the excitation of IDT-1. It contains an analog phase shifter to create a phase shift between the 2 IDTs electrical signal input. This allows to continuously tuning the SSAW pressure node along the channel width. Whereas the second line (downer one) is used for the excitation of IDT-2. Since the phase-shift response is not linear, the electric signal amplitude in the IDT-1 input might be different from those for IDT-2. That is why we use an attenuator in the bottom line to balance the electrical signal amplitude at the inputs of both IDT-1 and IDT-2.

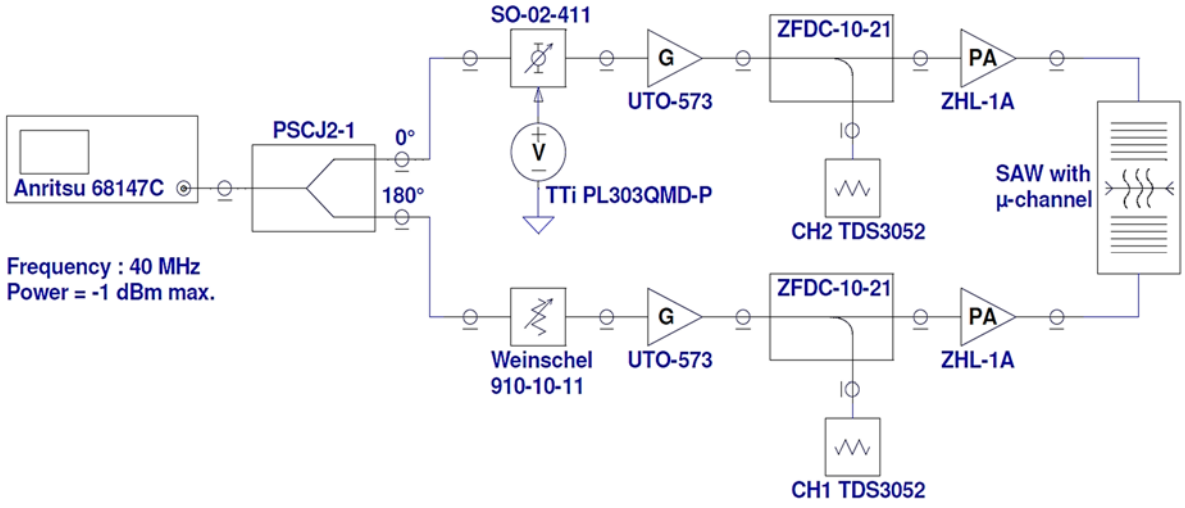

Fig. 8. Electronic circuit for the excitation of SAW interdigital transducer for the submicron acousto-fluidic sorting device.

For radio-frequency (RF) circuit analysis, the scattering parameters is widely used. The network analyzer commonly used for SAW device characterization. In fact, this makes it possible to measure insertion losses, rejection, bandwidth and the frequency of resonance of the SAW system.

Fig. 9 shows the insertion loss and reflection coefficient as a function of the frequency under these conditions. We can see that the central frequency: f_0 is 39.8 MHz which is very close to the simulation (40 MHz). The bandwidth is about 2 MHz, the loss of insertion is 30 dB and the rejection is 15 dB. Even if those parameters are not optimal, we were able to generate SSAW capable to drive submicron particles.

When the SAW system resonance frequency is determined, we can proceed with the optimization of the circuit by adding an electronic stage for an impedance matching of the IDTs by using the smith chart. The impedance between the RF source to the IDT electrodes need to be matched to maximize the electrical-mechanical energy transfer.

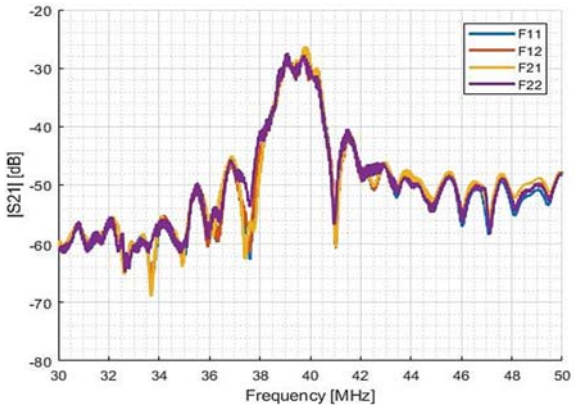

Fig. 9. Frequency response of the SAW interdigital transducer onto a 128° Y-cut $LiNb0_3$ substrate (for four identical devices F11, F12, F21 and F22). The central frequency f_0 = 39.8 MHz. The bandwidth is about 2 MHz, the loss of insertion is 30 dB and the rejection is 15 dB.

4.4. Microfluidic Measurements

In the following experiment, fluorescent calibration beads (480 nm in diameter/polymer) will be used to show the influence of surface stationary wave on submicron particles. We used a submicron synthetized beads from Micro particles GMBH®: MF-FITC-COOH, fluorescent beads (abs/em: 506/529 nm) with the diameter of 480 nm. These beads present carboxylic acid function allowing protein grafting on their surface, which permit to perform immunocapture, after sorting and recovery of particles.

Before introducing beads in microchannel, several conditioning steps are performed in the device: we wet the channel by using a water/methanol solution (50/50). The running buffer was PBS solution (Phosphate buffered saline) with Tween™ 20 (0.1 % v/v) from Thermo Fischer for a better wettability. To control the flow, the MFCS-EZ system from Fluigent® was used. The system allows the injection of sample in the microfluidic circuit depending on the pressure, from 0 to 1 bar but the working pressure was around 20 mbar. The experiment was monitored in real time by using a fluorescent microscope (AXIO SIP61023, ZEISS®).

5. Discussion

Fig. 10 presents a first analysis showing a laminar flow in the microchannel.

Initially, when we introduce nanoparticles in the inlet 1, it is automatically that the all particles exit from outlet 1. The beads are randomly dispersed along the half-channel in dynamic fluidic mode [28].

On the other hand, when we activate SAW with a normally phase–shifting of 180° between the IDTs, the randomly dispersed beads are aligned in a narrow line along the channel. This line is situated in the middle of the channel width which correspond to the pressure node position in the normally case (without supplementary phase-shifting) (cf. Fig. 11).

By shifting the SSAW phase with a relative phase shifting ranging from 0 to 180°, we translate beads from outlet 2 to outlet 1 or 3 according to the phase-shift we apply. As so, we realize sorting by driving 480 nm in diameter particles to one of the three channel outlets (Fig. 11). This is the first result showing that we can control vesicles flow and destination in specific outlet, just by acting on the phase of SSAW, to drive them from one side to other side.

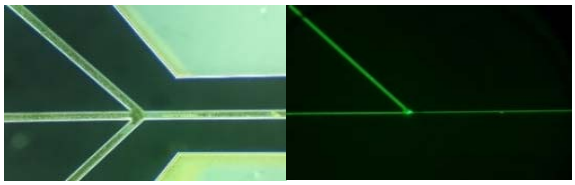

Fig. 10. Laminar flow experimentation using 480 nm in diameter beads in a buffer flowing throw a 60 µm of width fluidic channel: (left) optical view and (right) fluorescence microscopy images.

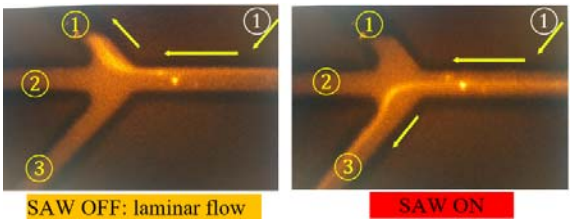

Fig. 11. Nanoparticles manipulation results using nanoparticles of 480 nm in the inlet 1. When we apply the SAW, we can move the particles from outlet 1 to outlet 2 or to outlet 3 according to the phase-shift we apply.

6. Conclusion

The main idea of this project is to be able to manipulate and sort the nanoscale vesicles by acoustic waves.

In this work, we experimentally validate the submicron particles alignment and sorting using SSAW microsystem. Experience has shown a submicron particles alignment at a fixed position along the channel. By shifting the SSAW phase, we can drive particles to one of the three outlets.

We have successfully fabricate an acoustic-based glass microfluidic system for label-free and continuous sorting of NP. We experimentally validated the particle manipulation and sorting using one type of 480 nm particles in glass microchannels. We validate the new concept of standing wave monitoring using phase-shifting.

By controlling the radiation force, a large number of particles can be manipulated in the same time. In fact, if a multiple particle sizes are presented in a continuous flow, each particle species of same size could be driven to one of the multiple microfluidic outlets.

Acknowledgements

This work is funded in part by NPRP grant # NPRP10-0201-170315 from the Qatar National Research Fund (a member of Qatar Foundation) and through the EIPHI Graduate School (contract "ANR-17-EURE-0002"). The authors also acknowledge the support of FEMTO-ST technological and characterization facilities. The findings herein reflect the work, and are solely the responsibility of the authors.

References

[1]. WU Mengxi, OZCELIK Adem, RUFO Joseph, *et al*., Acoustofluidic separation of cells and particles, *Nature Microsystems & Nanoengineering*, Vol. 5, Issue 1, 2019, p. 32.

[2]. Ferrara Katherine, Pollard Rachel, Borden Mark, Ultrasound microbubble contrast agents: fundamentals and application to gene and drug delivery, *Annu. Rev. Biomed. Eng.*, Vol. 9, 2007, pp. 415-447.

[3]. WU Junru, Acoustical tweezers, *The Journal of the Acoustical Society of America*, Vol. 89, Issue 5, 1991, pp. 2140-2143.

[4]. BLACK Justin P., WHITE Richard M., GRATE Jay W., Microsphere capture and perfusion in microchannels using flexural plate wave structures, in *Proceedings of the IEEE Ultrasonics Symposium, Munich,* Vol. 1, 2002, pp. 475-479.

[5]. HAAKE Albrecht, NEILD Adrian, RADZIWILL Gerald, *et al.*, Positioning, displacement, and localization of cells using ultrasonic forces. *Biotechnology and Bioengineering,* Vol. 92, Issue 1, 2005, pp. 8-14.

[6]. LEE Jungwoo, TEH Shia-Yen, LEE Abraham, *et al*., Single beam acoustic trapping, *Applied Physics Letters*, Vol. 95, Issue 7, 2009, p. 073701.

[7]. SHI Jinjie, AHMED Daniel, MAO Xiaole, *et al*., Acoustic tweezers: patterning cells and microparticles using standing surface acoustic waves (SSAW), *Lab on a Chip,* Vol. 9, Issue 20, 2009, pp. 2890-2895.

[8]. LENSHOF Andreas, MAGNUSSON Cecilia, LAURELL Thomas, Acoustofluidics 8: Applications of acoustophoresis in continuous flow microsystems, *Lab on a Chip*, Vol. 12, Issue 7, 2012, pp. 1210-1223.

[9]. ASHKIN Arthur, DZIEDZIC James M., Optical trapping and manipulation of viruses and bacteria, *Science,* Vol. 235, Issue 4795, 1987, pp. 1517-1520.

[10]. MACDONALD Michael P., PATERSON Lynn, VOLKE-SEPULVEDA K., *et al*., Creation and manipulation of three-dimensional optically trapped structures, *Science,* Vol. 296, Issue 5570, 2002, pp. 1101-1103.

[11]. FAZAL Furqan M., BLOCK Steven M., Optical tweezers study life under tension, *Nature Photonics*, Vol. 5, Issue 6, 2011, pp. 318-321.

[12]. THOMPSON Jeffrey Douglas, TIECKE T. G., DE LEON Nathalie P., *et al*., Coupling a single trapped atom to a nanoscale optical cavity, *Science,* 2013, Vol. 340, Issue 6137, pp. 1202-1205.

[13]. ZHONG Min-Cheng, WEI Xun-Bin, ZHOU Jin-Hua, *et al*., Trapping red blood cells in living animals using optical tweezers, *Nature Communications*, Vol. 4, 2013, p. 1768.

[14]. JUAN Mathieu L., GORDON Reuven, PANG Yuanjie, *et al*., Self-induced back-action optical trapping of dielectric nanoparticles, *Nature Physics*, Vol. 5, Issue 12, 2009, p. 915-919.

[15]. MANDAL Sudeep, SEREY Xavier, ERICKSON David, Nanomanipulation using silicon photonic crystal resonators, *Nano Letters*, Vol. 10, Issue 1, 2009, pp. 99-104.

[16]. PANG Yuanjie, GORDON Reuven, Optical trapping of a single protein, *Nano Letters*, Vol. 12, Issue 1, 2011, pp. 402-406.

[17]. YANG Allen HJ, MOORE Sean D., SCHMIDT Bradley S., *et al*., Optical manipulation of nanoparticles and biomolecules in sub-wavelength slot waveguides, *Nature*, Vol. 457, Issue 7225, 2009, pp. 71-75.

[18]. DING Xiaoyun, LIN Sz-Chin Steven, KIRALY Brian, *et al*., On-chip manipulation of single microparticles, cells, and organisms using surface acoustic waves, in *Proceedings of the National Academy of Sciences,* Vol. 109, Issue 28, 2012, p. 11105-11109.

[19]. SONG Dongli, YANG Dawei, POWELL Charles A., *et al*., Cell–cell communication: old mystery and new opportunity, *Cell Biology and Toxicology,* Vol. 35, Issue 2, 2019, pp. 89-93.

[20]. HUANG-DORAN Isabel, ZHANG Chen-Yu, VIDAL-PUIG Antonio, Extracellular vesicles: novel mediators of cell communication in metabolic disease, *Trends in Endocrinology & Metabolism*, Vol. 28, Issue 1, 2017, pp. 3-18.

[21]. HAAKE Albrecht, NEILD Adrian, RADZIWILL Gerald, *et al*., Positioning, displacement, and localization of cells using ultrasonic forces, *Biotechnology and Bioengineering*, Vol. 92, Issue 1, 2005, pp. 8-14.

[22]. COLLINS David J., MORAHAN Belinda, GARCIA-BUSTOS Jose, *et al*., Two-dimensional single-cell patterning with one cell per well driven by surface

acoustic waves, *Nature Communications*, Vol. 6, 2015, p. 8686.
[23]. LEE Kyungheon, SHAO Huilin, WEISSLEDER Ralph, *et al*., Acoustic purification of extracellular microvesicles, *ACS Nano*, Vol. 9, Issue 3, 2015, pp. 2321-2327.
[24]. GRÖSCHL Martin, Ultrasonic separation of suspended particles - Part I: Fundamentals, *Acta Acustica United with Acustica*, Vol. 84, Issue 3, 1998, pp. 432-447.
[25]. JOHANSSON Linda, ENLUND Johannes, JOHANSSON Stefan, *et al*., Surface acoustic wave induced particle manipulation in a PDMS channel—principle concepts for continuous flow applications, *Biomedical Microdevices*, Vol. 14, Issue 2, 2012, pp. 279-289.
[26]. CHARATI S. G., STERN S. A., Diffusion of gases in silicone polymers: molecular dynamics simulations, *Macromolecules*, Vol. 31, Issue 16, 1998, pp. 5529-5535.
[27]. HASHIMOTO Ken-Ya, HASHIMOTO Ken-Ya, Surface acoustic wave devices in telecommunications, *Springer-Verlag Berlin Heidelberg*, 2000.
[28]. A. Chaalane, D. Guneysu, M. Addouche, R. Zeggari, F. Lardet-Vieudrin, C. Elie-Caille, W. Boireau, A. Khelif, Continuous sorting of submicron particles in a pre-analytical device based on acousto-fluidic microsystem, in *Proceedings of the 5th International Conference on Sensors Engineering and Electronics Instrumentation Advances (SEIA'2019)*, Tenerife, (Canary Islands), Spain, September 2019, pp. 25-27.